

# Isolation and Structural Characterization of $[P(\text{AuPPh}_3)_5][\text{BF}_4]_2$ via Cleavage of a P–P Bond by Cationic Gold Fragments: Direct Evidence of the Structure of the Elusive Tetrakis[phosphineaurio(I)]phosponium(+) Cation

Robert E. Bachman and Hubert Schmidbaur\*

Anorganisch-chemisches Institut der Technischen Universität München, Lichtenbergstrasse 4, D-85747 Garching, Germany

Received July 28, 1995

## Introduction

Over the past decade interest in compounds containing gold(I) fragments has grown steadily.<sup>1</sup> One reason for this interest is the isolobal analogy between protons, carbonium ions, and  $[\text{LAu}(\text{I})]^+$  fragments (L = 2 electron donor). This analogy can be seen easily by comparing isostructural pairs of compounds such as  $[\text{R}_3\text{O}]^{+2}$  and  $[(\text{Ph}_3\text{PAu})_3\text{O}]^{+3}$  or  $[\text{R}_4\text{N}]^+$  and  $[(\text{Ph}_3\text{PAu})_4\text{N}]^{+4}$  (R = H, alkyl, aryl). However, as powerful as the isolobal analogy is, there are several notable exceptions such as the unusual square pyramidal geometry observed for  $[\text{As}(\text{AuPPh}_3)_4]^{+5}$  rather than the expected tetrahedral geometry based on comparison with all other known examples of arsonium cations. Other intriguing exceptions are the stability of the hypercoordinate species  $[\text{C}(\text{AuPPh}_3)_5]^+$ ,<sup>6</sup>  $[\text{C}(\text{AuPPh}_3)_6]^{2+}$ ,<sup>7</sup> and  $[\text{N}(\text{AuPPh}_3)_5]^{2+}$ ,<sup>8</sup> for which no analogous compounds based on organic fragments exist, and the instability of  $[\text{P}(\text{AuL})_4]^+$ , for which countless examples based on organic fragments exist. It is now recognized that the stability of these exceptional compounds is due to energetically favorable interactions between the formally closed shell ( $d^{10}$ ) gold atoms. This interaction, often referred to as aurophilicity, has been shown theoretically to arise from relativistic and correlation effects.<sup>9,10</sup>

As part of our continuing studies into the ability of  $[\text{LAu}(\text{I})]^+$  fragments to form novel main-group centered, electron-deficient clusters, we were interested in examining the use of species such as  $\text{P}_2(\text{SiMe}_3)_4$  as synthons. It was hoped that larger clusters centered by a dinuclear main-group fragment could be produced in this way. However, we have observed that the P–P bond in this compound is cleaved during the reaction to produce

**Table 1.** Data Collection and Refinement Parameters for  $[\text{I}][\text{BF}_4]_2 \cdot 3\text{CH}_2\text{Cl}_2^a$

empirical formula:	$\text{C}_{93}\text{H}_{81}\text{Au}_5\text{B}_2\text{Cl}_6\text{F}_8\text{P}_6$
fw =	2755.7
space group:	$P2_1/c$ (No. 14)
cell dims:	
<i>a</i> =	26.399(5) Å
<i>b</i> =	14.879(3) Å
<i>c</i> =	24.044 (5) Å
$\beta$ =	91.71(3)°
volume =	9440(5) Å <sup>3</sup>
Z =	4
F(000) =	5232
temp =	211 K
no. of indep reflns collcd:	15667 ( $R_{\text{int}} = 0.00$ )
no. of obsd reflns:	11855 ( $F > 4\sigma F$ )
no. of refined params:	1026
<i>R</i> =	4.43%
<i>R</i> <sub>w</sub> =	3.89%
goodness of fit:	1.56

<sup>a</sup>  $R = \sum |F_o - F_c| / \sum F_o$ ;  $R_w = [\sum w|F_o - F_c|^2 / w(F_o)^2]^{1/2}$ ;  $\text{GOF} = [\sum w|F_o - F_c|^2 / (M - N)]^{1/2}$ ; *M* = number of observed reflections, *N* = number of parameters and  $w = [\sigma^2(F_o) + 0.000124F_o^2]^{-1}$ .

$[\text{P}(\text{AuPPh}_3)_5]^{2+11}$  as the sole isolated product. Interestingly, the structural characterization of this cluster revealed a square pyramidal arrangement of the gold atoms in contrast to the trigonal bipyramidal structure expected by classical bonding arguments and in analogy with the previously characterized nitrogen analog.<sup>8</sup>

## Experimental Procedures

**General Considerations.** All reactions were carried out in oven-dried glassware using standard inert atmosphere techniques on a Schlenk line or in a drybox. Solvents were dried over the appropriate agents and distilled under nitrogen prior to use. <sup>31</sup>P NMR data were measured on a JOEL GX 400 at –75 °C and referenced to an external standard of 85% aqueous H<sub>3</sub>PO<sub>4</sub>.  $[(\text{Ph}_3\text{PAu})_3\text{O}][\text{BF}_4]$ <sup>3</sup> and  $\text{P}_2(\text{SiMe}_3)_4$ <sup>12</sup> were prepared according to literature procedures.

**Synthesis of  $[\text{P}(\text{AuPPh}_3)_5][\text{BF}_4]_2$ ,  $[\text{I}][\text{BF}_4]_2$ .** A solution of  $\text{P}_2(\text{SiMe}_3)_4$  in pentane was prepared by dissolving 200 mg of  $\text{P}_2(\text{SiMe}_3)_4$  (0.56 mmol) in 10 mL of pentane.  $[(\text{Ph}_3\text{PAu})_3\text{O}][\text{BF}_4]$  (0.50 g, 0.34 mmol) and 1.0 g of NaBF<sub>4</sub> were dissolved/suspended in a mixture of 35 mL of CH<sub>2</sub>Cl<sub>2</sub> and 15 mL of THF, and the resulting mixture was cooled to –10 °C. A 3.0 mL (0.17 mmol) aliquot of the  $\text{P}_2(\text{SiMe}_3)_4$  solution was then added in one portion via syringe. The stirred reaction mixture slowly turned an orange-yellow color as it was allowed to warm to room temperature overnight. The reaction mixture was filtered to remove the insoluble material (primarily excess NaBF<sub>4</sub>) and the crude product isolated as a yellow powder by the addition of a large amount of pentane (50–75 mL). X-ray quality crystals were grown by the gas phase diffusion of ethyl ether into a solution of  $[\text{I}][\text{BF}_4]_2$  in CH<sub>2</sub>Cl<sub>2</sub>. Yield: 0.32 g (38% based on phosphorus). <sup>31</sup>P NMR: (CD<sub>2</sub>Cl<sub>2</sub>, –75 °C, ppm) 38.4 d (<sup>2</sup>*J*<sub>pp</sub> = 186 Hz), –123.3 h (<sup>2</sup>*J*<sub>pp</sub> = 186 Hz); (CD<sub>2</sub>Cl<sub>2</sub>, 20 °C, ppm) 40.6 d (<sup>2</sup>*J*<sub>pp</sub> = 186 Hz), –120.5 br. MS: (FAB, NBA) 2413, 1865, 1604, 1342, 1080, 721, 459; (FD, CH<sub>2</sub>Cl<sub>2</sub>) 1163, 721, 459 Anal. Calcd (found) for  $\text{C}_{90}\text{H}_{75}\text{Au}_5\text{B}_2\text{F}_8\text{P}_6$ : C, 43.2 (42.8); H, 3.02 (3.07); Au, 39.4 (39.2)

**X-ray Crystallography.** A red brown crystal of  $[\text{I}][\text{BF}_4]_2 \cdot 3\text{CH}_2\text{Cl}_2$  was mounted in a glass capillary tube under argon and examined on an Enraf-Nonius CAD4 diffractometer using graphite monochromated Mo K<sub>α</sub> radiation ( $\lambda = 0.71069$  Å). The data collection and refinement parameters are summarized in Table 1. The data were corrected for Lorenz and polarization effects as well as for absorption using an empirical correction based on  $\psi$ -scans. All computations were

- (1) Schmidbaur, H. *Gold Bull.* **1990**, 23, 11.
- (2) Meerwein, H.; Heinz, G.; Hofmann, P.; Kronig, E.; Pfeil, E. *J. Prakt. Chem.* **1937**, 147, 257.
- (3) Nesmeyanov, A. N.; Grandberg, K. I.; Dyadchenko, V. P.; Lemenovskii, D. A.; Perevalova, E. G. *Izv. Akad. Nauk. SSSR, Ser. Khim.* **1974**, 740.
- (4) Slovokhotov, Yu. L.; Struchkov, Yu. T. *J. Organomet. Chem.* **1984**, 277, 143. Perevalova, E. G.; Smyslova, E. I.; Dyadchenko, V. P.; Grandberg, K. I.; Nesmeyanov, A. N. *Izv. Akad. Nauk. SSSR, Ser. Khim.* **1980**, 1455. Brodbeck, A.; Strähle, J. *Acta Crystallogr.* **1990**, A46, C 232.
- (5) Zeller, E.; Beruda, H.; Kolb, A.; Bissinger, P.; Riede, J.; Schmidbaur, H. *Nature* **1991**, 352, 141.
- (6) Scherbaum, F.; Grohmann, A.; Müller, G.; Schmidbaur, H. *Angew. Chem.* **1989**, 101, 464; *Angew. Chem., Int. Ed. Engl.* **1989**, 28, 463.
- (7) Scherbaum, F.; Grohmann, A.; Huber, B.; Krüger, C.; Schmidbaur, H. *Angew. Chem.* **1988**, 100, 1602; *Angew. Chem., Int. Ed. Engl.* **1988**, 27, 1544.
- (8) Grohmann, A.; Riede, J.; Schmidbaur, H. *Nature* **1990**, 345, 140.
- (9) Görling, A.; Rösch, N.; Ellis, D. E.; Schmidbaur, H. *Inorg. Chem.* **1991**, 30, 3986. Haerberlen, O. D.; Schmidbaur, H.; Rösch, N. *J. Am. Chem. Soc.* **1994**, 116, 8241.
- (10) Li, J.; Pyykkö, P. *Inorg. Chem.* **1993**, 2630. Li, J.; Pyykkö, P. *Chem. Phys. Lett.* **1992**, 197, 586.

- (11) Schmidbaur, H.; Weidenhiller, G.; Steigelmann, O. *Angew. Chem.* **1991**, 103, 442. *Angew. Chem., Int. Ed. Engl.* **1991**, 30, 433.
- (12) Schumann, H.; Rösch, L.; Schmidt-Fritsche, W. *Chem. Ztg.* **1977**, 101, 156.

carried out with the SHELXTL-PC package.<sup>13</sup> The initial structure solution was performed with direct methods which located all five gold atoms. The remaining non-hydrogen atoms were then located by successive Fourier syntheses. The final refinement was carried out in blocks with all the non-hydrogen atoms of the cation refined anisotropically and the remaining non-hydrogen atoms refined isotropically. Hydrogen atoms were included in calculated positions for the cation only using a standard riding model. The function minimized during refinement was  $R_w = [\sum |F_o - F_c|^2 / w(F_o)^2]^{1/2}$  with  $w = [\sigma^2(F_o) + 0.000124F_o^2]^{-1}$ . Due to disorder problems with the anions, they were refined as rigid tetrahedra with two sets of atomic positions for each anion.

## Results

The reaction of  $P_2(SiMe_3)_4$  with  $[(Ph_3PAu)_3O]BF_4$  in the presence of excess  $NaBF_4$  produces a bright orange-yellow solution from which  $[1][BF_4]_2$  can be isolated. This compound has been previously synthesized by the reaction of  $P(SiMe_3)_3$  with the same gold salt in low yields.<sup>11</sup> The rupture of the P–P bond observed here is consistent with that seen in other systems containing dinuclear group 16 fragments (S–S and Te–Te).<sup>14,15</sup> FABMS reveals a signal at 2413 as the highest peak, consistent with the presence of  $[1][BF_4]^+$ . The next signal at 1865 corresponds to the loss of one  $[Ph_3PAu]^+$  fragment and the  $[BF_4]^-$  counterion to produce the hypothetical species  $[P(AuP-Ph_3)_4]^+$ . From this peak it is possible to observe only peaks corresponding to the loss of consecutive triphenylphosphine moieties with no further loss of gold. This observation agrees well with the results of a theoretical study which predicts a significant degree of stability for the bare  $[PAu_4]^+$  cation.<sup>10</sup>

X-ray quality crystals were obtained from a slow diffusion of ether vapor into a methylene chloride solution of  $[1][BF_4]_2$ . The monoclinic ( $P2_1/c$ , No. 14) crystals were shown to contain one cation, two anions, and three molecules of lattice  $CH_2Cl_2$  per asymmetric unit. There are no unusually short contacts between the cation and the anion, however there appear to be some weak interactions between the solvent molecules and the gold atoms of the cation with the Au–Cl contacts ranging from 3.6 to 3.9 Å.

The molecular structure of the cation is best described as a distorted square pyramid with four gold atoms forming the base of the pyramid and a unique gold atom residing at the apex (Figure 1 and Table 2). This geometry produces four short gold–gold contacts along the base of the pyramid ranging from 2.869(1) to 3.013(1) Å. These values are comparable to those seen in other clusters with aurophilic bonding.<sup>3,5–8</sup> As a consequence of the gold–gold contacts, the basal Au–P–Au angles ( $74.4(1)^\circ$  to  $79.2(1)^\circ$ ) at the central phosphorus are contracted from ideal. The P–Au bonds between the central P and the basal gold atoms range from 2.356(3) to 2.379(3) Å. In contrast, the Au–P bond between the cluster core and the unique apical gold (2.295(3) Å) is significantly shorter than those of the basal gold atoms. Furthermore, in opposition to the short-long P–Au–P bond length pattern seen at the basal gold atoms, the two P–Au bonds are of essentially equal length for this gold atom with an Au–P<sub>phosphine</sub> distance of 2.288(3) Å. The geometry in the square base of  $[1][BF_4]_2$  shows significant distortion from the ideal. Interestingly, a similar distortion is seen in the related system  $[(o\text{-tol})P(AuPPh_3)_4]^{2+}$  (Table 3).

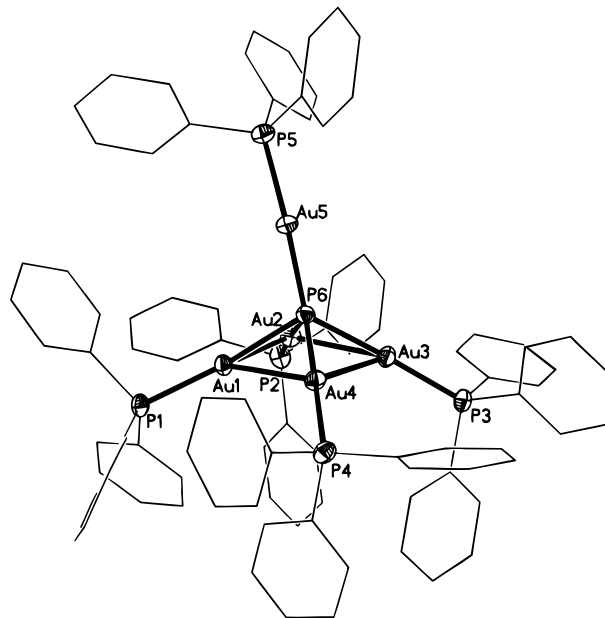


**Figure 1.** Molecular structure for the cation  $[1]^{2+}$  with the thermal ellipsoids shown at the 50% probability level. The phenyl rings have been drawn as outlines for clarity.

**Table 2.** Selected Bond Lengths (Å) and Angles (deg) for  $[1][BF_4]_2$

P(6)–Au(1)	2.375(2)	Au(1)–P(6)–Au(2)	75.2(1)
P(6)–Au(2)	2.379(3)	Au(1)–P(6)–Au(4)	74.4(1)
P(6)–Au(3)	2.356(3)	Au(2)–P(6)–Au(3)	78.0(1)
P(6)–Au(4)	2.370(3)	Au(3)–P(6)–Au(4)	79.2(1)
P(6)–Au(5)	2.295(3)	Au(5)–P(6)–Au(1)	109.4(1)
Au(1)–Au(2)	2.900(1)	Au(5)–P(6)–Au(2)	112.7(1)
Au(1)–Au(4)	2.869(1)	Au(5)–P(6)–Au(3)	130.3(1)
Au(2)–Au(3)	2.982(1)	Au(5)–P(6)–Au(4)	120.2(1)
Au(3)–Au(4)	3.013(1)	P(6)–Au(1)–P(1)	174.0(1)
Au(1)–P(1)	2.279(3)	P(6)–Au(2)–P(2)	177.9(1)
Au(2)–P(2)	2.294(3)	P(6)–Au(3)–P(3)	177.2(1)
Au(3)–P(3)	2.292(3)	P(6)–Au(4)–P(4)	176.5(1)
Au(4)–P(4)	2.283(3)	P(6)–Au(5)–P(5)	176.0(1)
Au(5)–P(5)	2.288(3)		

**Table 3.** Comparative Bond Lengths (Å) and Angles for the Square Pyramidal Cores of  $[1]^{2+}$  and  $[(o\text{-tol})P(AuPPh_3)_4]^{2+}$

	$[1]^{2+}$	$[(o\text{-tol})P(AuPPh_3)_4]^{2+}$
Au–Au	2.869(1)	2.891(1)
	2.900(1)	2.975(1)
	2.982(1)	2.984(1)
	3.013(1)	3.012(1)
P–Au	2.356(3)	2.354(2)
	2.370(3)	2.357(2)
	2.375(2)	2.379(2)
	2.379(3)	2.379(2)
Au–P–Au	74.4(1)	75.3(1)
	75.2(1)	77.9(1)
	78.0(1)	78.2(1)
	79.2(1)	79.0(1)

Since these two systems crystallize in different space groups with significantly different packing arrangements including differences in the types and amounts of lattice solvent present, it is unlikely that the distortions are due to packing effects.

The structure of  $[1][BF_4]_2$  also provides an opportunity to gain some qualitative experimental insight into the strength of the Au–Au aurophilic interaction as a function of distance. In the hypothetical trigonal bipyramidal structure, there would be six interactions at approximately 3.35 Å (based on the experimentally observed average P–Au distance of 2.37 Å) and three longer interactions of 4.10 Å which can be neglected. In the square pyramidal structure there are only 4 interactions of 2.94

(13) SHELXTL PC v 4.2, Siemens Crystallographic Research Systems, Madison, WI, 1990.

(14) Jones, P. G.; Sheldrick, G. M.; Hadicke, E. *Acta Crystallogr.* **1980**, *B36*, 2777. Wang, S.; Fackler, J. P. Jr. *Inorg. Chem.* **1990**, *29*, 4404.

(15) Schultz Lang, E.; Maichle-Mössmer, C.; Strähle, J. *Z. Anorg. Allg. Chem.* **1994**, *620*, 1678.

(16) Schmidbaur, H.; Zeller, E.; Weidenhiller, G.; Steigelmann, O.; Beruda, H. *Inorg. Chem.* **1992**, *31*, 2370.

Å. This difference implies that as the Au–Au distance increases from 2.94 to 3.35 Å, the attractive interaction must decrease quite significantly.

The square pyramidal geometry seen in this study contrasts directly with the trigonal bipyramidal structure proposed earlier<sup>11</sup> on the basis of a low temperature (–75 °C) solution <sup>31</sup>P NMR data which indicated that all five peripheral gold atoms are equivalent under the conditions employed. We undertook a careful reinvestigation of these NMR results using single crystalline material. The present study reconfirmed the essential findings of the earlier observations. At –75 °C the spectrum consists of a doublet at 38.4 ppm for the phosphines and a sextet at –123.3 ppm (<sup>2</sup>J<sub>pp</sub> = 186 Hz) for the central phosphorus atom. At room temperature the splitting at the central phosphorus atom collapses to an ill-defined broad multiplet while the doublet observed for the phosphine signal is maintained. Additionally, if a trace of extra triphenylphosphine is present in the solution, the phosphine doublet collapses to a singlet and shifts to 41.6 ppm, and the center phosphorus signal shifts from –122 to –98 ppm and grows even broader. These signals are essentially identical to those reported previously for the novel species [(Ph<sub>3</sub>PAu)<sub>4</sub>P{Au(PPh<sub>3</sub>)<sub>2</sub>}]<sup>2+</sup>.<sup>17</sup> When the mixed Ph<sub>3</sub>P–[1]<sup>2+</sup> system is cooled to –75 °C, two sets of doublets appear in the phosphine region at 40.6 and 38.9 ppm. The central phosphorus signal remains at –98 ppm as a very broad featureless signal. The best interpretation of these data relies on two independent scrambling processes. At room temperature there is some degree of intermolecular exchange between the two clusters. On the basis of the acceleration in the rate of this exchange which occurs in the presence of extra free phosphine, it is most likely that this process involves the exchange of phosphines; however, exchange of intact [LAu]<sup>+</sup> fragments can not be completely ruled out. When the temperature is lowered to –75 °C for the pure sample, this exchange process is stopped leaving only an intramolecular scrambling of the five LAu moieties via a facile Berry pseudorotation process. As a result of halting the intermolecular exchange process, the central phosphorus signal is shifted to higher field and is transformed into a well-resolved sextet. When excess phosphine is present in solution, the intermolecular exchange process continues even at low temperature resulting in the observed ill-resolved spectrum. Unfortunately, since pseudorotation makes the square-pyramidal

and trigonal bipyramidal forms equivalent, the exact structure of the cation in solution remains unclear.

### Discussion

The synthesis of [1][BF<sub>4</sub>]<sub>2</sub> represents the first example to our knowledge of the cleavage of a P–P bond by cationic gold fragments. Structurally, [1][BF<sub>4</sub>]<sub>2</sub> is another example of a cluster made of gold(I) units which violates the classical rules of bonding and structure. It also represents a rare structurally characterized example of a homoleptic gold cluster centered by phosphorus and the first without sterically demanding ligands, the only other homoleptic species being the cation [P(AuP<sup>t</sup>Bu<sub>3</sub>)<sub>4</sub>]<sup>+</sup>.<sup>18</sup>

[P(AuP<sup>t</sup>Bu<sub>3</sub>)<sub>4</sub>]<sup>+</sup> was found to display tetrahedral geometry rather than square pyramidal expected on the basis of theoretical work.<sup>10</sup> However, closer examination reveals that in this case the structure is imposed by the steric constraints of the *tert*-butyl groups. The question therefore still remains as to the structure of the [P(AuPR<sub>3</sub>)<sub>4</sub>]<sup>+</sup> cation in the absence of these sterically forcing ligands. By comparison with the previously characterized<sup>8</sup> trigonal bipyramidal cluster [N(AuPPh<sub>3</sub>)<sub>5</sub>]<sup>2+</sup>, which contains a smaller main-group element at its center, it can be seen that there are no steric reasons for the deviation of [1][BF<sub>4</sub>]<sub>2</sub> from the expected trigonal bipyramidal geometry. It is therefore safe to assume that the observed geometry is due to other energetic factors, such as the aurophilic interactions present in the square base. Furthermore, [1]<sup>2+</sup> can be viewed as being composed of a [P(AuPPh<sub>3</sub>)<sub>4</sub>]<sup>+</sup> cluster which binds to a strong electron acceptor, [Ph<sub>3</sub>PAu]<sup>+</sup>. Thus, the unexpected structure of [1][BF<sub>4</sub>]<sub>2</sub> suggests very strongly that the structure of the elusive [P(AuPR<sub>3</sub>)<sub>4</sub>]<sup>+</sup> cation is indeed square pyramidal.

**Acknowledgment.** This work was supported by the Deutsche Forschungsgemeinschaft and by the Fonds der Chemischen Industrie. Further support was given by Degussa AG and Heraeus GmbH in the form of donated chemicals. The authors would like to thank Mr. J. Riede for establishing the X-ray data set. R.E.B. would also like to thank the Alexander von Humboldt Stiftung for a Fellowship.

**Supporting Information Available:** Tables giving full details of the crystal structure determination including fractional atomic coordinates, isotropic and anisotropic displacement parameters, and full bond metrical data (15 pages). Ordering information is given on any current masthead page.

IC950946N

(17) Beruda, H.; Zeller, E.; Schmidbaur, H. *Chem. Ber.* **1993**, *126*, 2037.

(18) Zeller, E.; Beruda, H.; Schmidbaur, H. *Chem. Ber.* **1993**, *126*, 2033.